

## Computational Approaches for Tortuosity Determination in 3D Structures

E. Solórzano<sup>1</sup>, S. Pardo-Alonso<sup>1</sup>, L. Brabant<sup>3</sup>, J. Vicente<sup>2</sup>, L. Van Hoorebeke<sup>3</sup> M.A. Rodríguez-Pérez<sup>1</sup>

<sup>1</sup>CellMat Laboratory, Condensed Matter Physics Department, University of Valladolid, Paseo de Belén, 7 47011, Valladolid [email: [esolo@fmc.uva.es](mailto:esolo@fmc.uva.es)]

<sup>2</sup>Laboratoire IUSTI, CNRS UMR 7343, Aix Marseille Université, France

<sup>3</sup>UGCT, Department of Physics and Astronomy, Faculty of Sciences, Proeftuinstraat 86 9000 Ghent, Belgium

**Keywords:** cellular materials, tortuosity, transport properties, geodesic distance

### ABSTRACT

Tortuosity is a parameter of key importance to study transport properties in either solid phase (thermal, electrical) and/or fluid phase (acoustics, mass/heat flow, etc). This structure-related parameter expresses mathematically the real pathway distance in comparison to the straightest one when travelling along certain direction through the material's internal structure.

Tortuosity determination is not reliable in 2D and needs to be computed in 3D structures. However, computation of 3D algorithms in complex structures is not an easy task. This work discusses two methodological approaches based on their correspondent computation algorithms working on a collection of 3D tomography data sets of different cellular materials. The tortuosity analysis is carried out in both solid and fluid phases. Results will be compared and correlated. A detailed discussion in terms of these models and the materials will be given.

### 1. INTRODUCTION

Transport properties in porous materials are strongly determined by morphology and particularly by the tortuous path in both solid and gaseous (fluid) phases (Brun 2010, Gommes *et al.* 2009, Hugo 2012). The parameter expressing this tortuous path is named tortuosity. As a consequence, the evaluation of this parameter is of an extraordinary importance but it is also difficult to be determined. This parameter contributes significantly to improve the accuracy of physical models related to transport throughout the continuous solid phase. On the other hand, others properties such permeability, flow resistance or diffusivity are connected to the gaseous phase topology and, again, models consider an adjustable factor (tortuosity) that frequently needs to be indirectly determined from a dataset after proper fitting. Other morphological factors such as the open cell content are related to the fluid-phase tortuosity since this parameter should change from a rather low value, when the material presents 100% connected cells, up to infinitum, when cells are closed below a certain threshold creating a discontinuous fluid phase and a vast majority of closed porosity material.

It is important to note that this concept is included within varying theoretical frames and diverse experimental determination procedures. Therefore, it creates an intrinsic difficulty for choosing a computational approach to be universally valid in any kind of material. Another difficulty associated to the determination of this 3D parameter is related to the computation complexity. In this sense, only in recent years it has been possible to perform these computations in high-performance –but rather conventional– CPUs. Furthermore there is a lack in the literature regarding computation techniques for these parameters and only a few existing works are focused on some practical methods for a particular set of materials (medical, geological, etc.) being frequently not so complex in comparison to cellular materials (Bullitt *et al.* 2003, Gommes *et al.* 2009).

## 2. MATERIALS AND METHODS

### 2.1. Materials

A collection of diverse cellular materials with varying degrees of solid/gaseous phase tortuosity has been selected to test the different computing procedures developed in this work. Three different samples of closed cell low-density polyethylene foam (LDPE) were used to compute solid phase tortuosity (fluid phase is mostly discontinuous/occluded in these materials). The computation of the solid phase tortuosity is expected to be related to the presence/absence of wrinkles in the cell walls. In addition, four open cell LDPE-EVA foams have been used to calculate the fluid phase tortuosity, the physical tortuosity in these materials was previously calculated by electric impedance method by using an electrolyte dissolution occupying the fluid phase. Finally, six open-cell aluminium foams produced by infiltration methods were used to determine both gaseous and solid phase tortuosity. Acoustic absorption on these materials (related to both solid and gaseous tortuosity) has been experimentally determined in parallel.

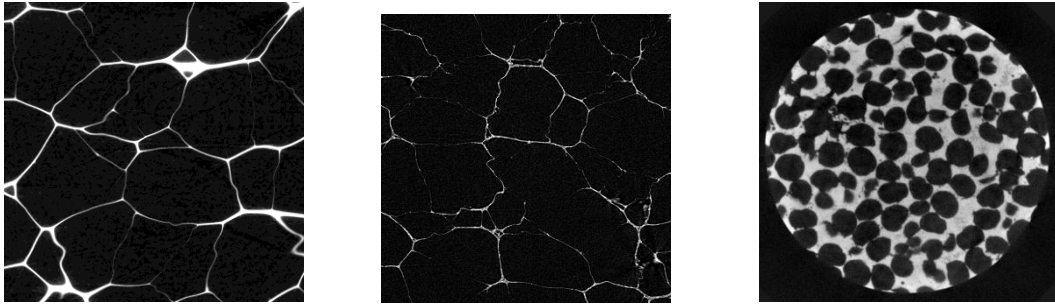


Figure 1: LDPE closed cell foam (left), LDPE-EVA open cell foam (center) and infiltrated metallic foam (right) tomograms.

The tomograms were acquired and reconstructed at different cone-beam X-ray scanners. Settings were optimized according to every sample peculiarity (density, material, sample size, structure thickness, etc.) obtaining a final pixel size in the range of 5-20 microns. Figure 1 show examples of the three types of materials analyzed.

### 2.2. Methods of analysis

The methods proposed in this section are self-developed algorithms that will be comparatively tested in these materials for the different phases. A description of each method is given in the following sections.

All methods are based on the definition of tortuosity as the ratio between geodesic distance (the path length through the cells) and the Euclidean distance (shortest straight distance, projection over the Cartesian axis), see eq.1. The geodesic distance includes the extra distance that has to be covered by “travelling” through the gaseous/solid phase.

$$\tau = \frac{\text{dist}_{\text{geodesic}}(p_1, p_2)}{\text{dir}(\|p_1 - p_2\|)} \quad (\text{eq.1})$$

It is important to note that tortuosity is a directional parameter; therefore we can obtain a value for each direction in the 3D space. Three principal directional values are commonly used and they correspond to the three Cartesian axes (X, Y and Z).

#### 2.2.1. Pore-throat-pore distances methods

This method consists of an iterative computational approach, determining the cumulative distance ratio in between pore-throat-pore distances and Euclidean distance. In this case the Euclidean distance is calculated in between two pore centres. It is compared with the summed distances of the centre of the first pore, the centre of mass of the pore interconnection (throat) and the centre of the second pore and the centre of mass of the same throat. In other words, the geodesic distance in this methodology is the distance of the pore-throat-pore track. The pore-throat-pore track is illustrated by the blue line in figure 2. This method was implemented in the Morpho+ software package (Brabant et

*a.l.* 2011). This method consisted in calculating the throats by first determining the Euclidean distance transform, and subsequently applying a watershed based separation (Vincent and Soille 1991) on the complement of this distance transform. Because the watershed based separation should separate objects at their narrowest point, the obtained watersheds can be used as throats.

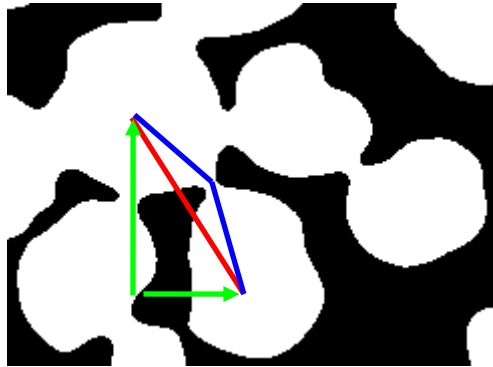


Figure 2: Scheme pore-interconnection-pore (blue) geodesic distances and Euclidean distance (red). The projections of the Euclidean distance on x-axis and y-axis are shown in green.

### 2.2.2. Fast Marching algorithm

The method in the Imorph package is a Fast Marching algorithm based on the fluid propagation technique and follows a different concept. It mainly consists in computation of a parallel fluid wave virtually travelling from certain point and propagating at virtual constant speed without intersecting any other pixel than those contained in the selected phase (Brun 2009). This procedure computes the virtual arrival time of the fluid at the end points in the final plane and calculates an average. This result is normalized by the arrival time obtained for a single-phase material and the ratio is directly outputted as a tortuosity value. The assumption is correct because during the process the virtual velocity has been kept constant and thus the delay directly corresponds to a higher distance tracked. This approach can be applied to both solid and fluid phases and is already implemented in Imorph.

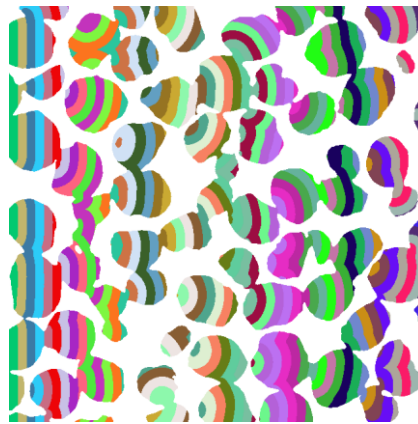


Figure 3: Wavefront propagation through the gaseous phase. The colour code corresponds to different times after the initial propagation.

## 3. RESULTS AND DISCUSSION

Table 1 shows preliminary results of tortuosity both in the solid and gaseous phase for both the fast marching algorithm and the pore-throat-pore distance methods implemented in Imorph and Morpho+ respectively. From these results it can be observed that the fast marching technique outputs values extremely low and, only in case of the solid network tortuosity with extremely narrow cells walls, the values are much below the expected one (approx. 15). On the other hand, the pore-throat-pore distances method provides higher values. Most of these values are congruent with the expected tortuosity although value for gaseous phase of open cell LDPE-EVA foam seems to be low in

comparison to the experimental value (approx. 15). In general, values obtained by the different methods are not comparable.

Tortuosity values are not the same in all the spatial directions and therefore it can be told that these materials are anisotropic. In fact, although it is not showed in this work, this anisotropy in tortuosity correlates with other structural foam features. In general, Z-axis of these materials (foaming direction) presents the higher tortuosity.

Table 1: *Tortuosity values*

Sample	Gaseous phase						Solid phase					
	Fast marching			Pore-throat-pore			Fast marching			Pore-throat-pore		
<i>Direction</i>	X	Y	Z	X	Y	Z	X	Y	Z	X	Y	Z
Close cell LDPE	---	---	---	---	---	---	1.0	1.7	2.0	2.0	2.2	2.5
							7	1	5	3	6	1
Open cell LDPE-EVA	1.02	1.0	1.0	2.0	2.1	2.2	1.0	1.0	1.0	2.2	2.6	2.0
		1	2	3	2	8	8	7	8	0	2	5
Metal foam	1.04	1.0	1.0	2.1	2.3	1.9	1.0	1.0	1.0	2.7	3.0	3.1
		3	3	4	0	9	2	1	2	5	6	8

#### 4. CONCLUSIONS AND FUTURE WORK

Two different computational approaches for the determination of tortuosity have been proposed and compared over a set of different porous materials. Current results point to mismatching values among different methods but further analysis needs to be done. In general, computed tortuosity is low in comparison with experimental results. A calibration of the geometrical values calculated from tomographies with experimental results will be further done.

#### 5. ACKNOWLEDGEMENTS

Financial support from the Spanish Ministry of Science and Innovation and FEDER (MAT2009-14001-C02-01 and MAT2012-34901), the European Spatial Agency (Project MAP AO-99-075), PIRTU contract of S. Pardo-Alonso by Junta of Castile and Leon (EDU/289/2011) co-financed by the European Social Fund and Juan de la Cierva contract of E. Solórzano by the Ministry of Economy and Competitiveness (JCI-2011-09775) are gratefully acknowledged. The Special Research Fund of the Ghent University (BOF) is acknowledged for the doctoral grant to Loes Brabant.

#### 6. REFERENCES

- Brabant L., Vlassenbroeck J., De Witte Y., Cnudde V., Boone M.N., Dewanckele J. and Van Hoorebeke L. (2011). Three-Dimensional Analysis of High-Resolution X-Ray Tomography Data with Morpho+. *Microscopy and Microanalysis*, 17(2), 252-263.
- Brun E. (2009). Thèse de doctorat, Université de Provence.
- Bullitt E., Gerig G., Pizer S. M., Lin W. and Aylward S.R. (2003). Measuring Tortuosity of the Intracerebral Vasculature From MRA Images. *IEEE Transactions on Medical Imaging*, 22(9), 1163-1171.
- Hugo J.M. (2012). Thèse de doctorat, Université d'Aix Marseille.
- Gommes C.J., Bons A.J., Blacher S., Dunsmuir J.H. and Tsou A.H. (2009). Practical Methods for Measuring the Tortuosity of Porous Materials from Binary or Gray-Tone Tomographic Reconstructions. *AIChE Journal*, 55(8), 2000-2012.
- Vincent L. and Soille P. (1991). Watersheds in digital spaces: an efficient algorithm based on immersion simulations. *IEEE Transactions on Pattern Analysis and Machine Intelligence*, 13(6), 583-598.